Adsorption Characteristics of 1,4-Phenylene Diisocyanide on Gold Nanoparticles: Infrared and Raman Spectroscopy Study

ARTICLE *in* LANGMUIR · JULY 2003

Impact Factor: 4.46 · DOI: 10.1021/la026756o

Adsorption Characteristics of 1,4-Phenylene Diisocyanide on Gold Nanoparticles: Infrared and Raman Spectroscopy Study

Hak Soo Kim, Seung Joon Lee, Nam Hoon Kim, Jae Keun Yoon, Hyoung Kun Park, and Kwan Kim*

Laboratory of Intelligent Interfaces, School of Chemistry and Molecular Engineering and Center for Molecular Catalysis, Seoul National University, Seoul 151-742, Korea

Received October 26, 2002. In Final Form: May 31, 2003

The adsorption characteristics of 1,4-phenylene diisocyanide (1,4-PDI) on colloidal Au particles have been investigated by means of various analytical techniques including infrared and Raman spectroscopy. Surface-enhanced infrared absorption spectroscopy as well as atomic force microscopy and quartz crystal microbalance clearly showed that 1,4-PDI should be adsorbed on gold via the carbon lone-pair electrons of one isocyanide group and that the pendent isocyanide group could react further with Au nanoparticles, suggesting that nanoarrayed electrodes could be fabricated using 1,4-PDI and Au nanoparticles. In the Au sol medium, the adsorption scheme was highly dependent on the concentration of 1,4-PDI. As a result, in the surface-enhanced Raman scattering (SERS) spectra, the relative peak intensity of the $\nu(NC)_{free}$ and $\nu(NC)_{bound}$ modes varied with a sigmoid shape with respect to the 1,4-PDI concentration. The inflection point (IP) seemed surprisingly to correspond to the monolayer-coverage limit. At lower concentration below the IP, 1,4-PDI appeared to be bonded exclusively to two different gold particles forming two Au−C bonds. The resulting fractal clusters were rather small-sized, however, probably due to the repulsive barrier between Au particles at lower concentration. In contrast, at higher concentration above the IP, a highly aggregated superstructure showing both the $\nu(NC)_{free}$ and $\nu(NC)_{bound}$ bands was readily formed. Altogether, the major driving force for Au nanoparticles to assemble large aggregates seemed to be the formation of two Au−C bonds per 1,4-PDI rather than the usual adsorbate-induced reduction of the electrical repulsive barrier between Au particles.

1. Introduction

In the past decade, the adsorption of organic molecules on metal surfaces, along with the derivatization of nanosized metal particles with organic molecules, has attracted tremendous research interest.[1,2] In addition to the fundamental interest in such metal adsorbate systems, practical considerations such as the modification of metal surfaces, and the preparation of organic thin films and nanostructured arrays have led to increased research activity in this area.[3−6] The most widely studied and well-characterized systems include thiols and disulfides on gold and silver and carboxylic acids on aluminum oxide and silver.[7−9] It has now been well-established that aliphatic as well as aromatic dithiols adsorb on gold as monothiolates by forming one single Au−S covalent bond. The other thiol group is pendent with respect to the gold surface.[10] Self-organization of gold nanoparticles onto a gold substrate can thus be achieved by the assembly of

* To whom all correspondence should be addressed. Telephone: +82-2-8806651. Fax: +82-2-8743704. E-mail: kwankim@plaza.snu.ac.kr.

(1) Ulman, A. *Chem. Rev.* **1996**, *96*, 1533.

(2) (a) Musick, M. D.; Keating, C. D.; Keefe, M. H.; Natan, M. J. *Chem. Mater.* **1997**, *9*, 1499. (b) Chen, S.; Ingram, R. S.; Hostetler, M. J.; Pietron, J. J.; Murray, R. W.; Schaaff, T. G.; Khoury, J. T.; Alvarez, M. M.; Whetten, R. L. *Science* **1998**, *280*, 2098. (c) Brust, M.; Bethell, D.; Kiely, C. J.; Schiffrin, D. J. *Langmuir* **1998**, *14*, 5425. (d) Musick, M. D.; Pena, D. J.; Botsko, S. L.; McEvoy, T. M.; Richardson, J. N.; Natan, M. J. *Langmuir* **1999**, *15*, 844.

(3) Swalen, J. D.; Allara, D. L.; Andrade, J. D.; Chandross, E. A.; Garoff, S.; Israelachvili, J.; MaCarthy, T. J.; Murray, R.; Pease, R. F.; Rabolt, J. F.; Wynne, K. J.; Yu, H. *Langmuir* **1987**, *3*, 932.

(4) Ulman, A., Ed. *Thin Films*; Academic Press: San Diego, CA, 1995.

(5) (a) Andres, R. P.; Bielefeld, J. D.; Henderson, J. I.; Janes, D. B.; Kolagunta, V. R.; Kubiak, C. P.; Mahoney, W. J.; Osifchin, R. G. *Science* **1996**, *273*, 1690. (b) Fendler, J. H. *Chem. Mater.* **1996**, *8*, 1616. (c) Grabar, K. C.; Allison, K. J.; Baker, B. E.; Bright, R. M.; Brown, K. R.; Freeman R. G.; Fox, A. P.; Keating, C. D.; Musick, M. D.; Natan, M. J. *Langmuir* **1996**, *12*, 2353. (d) Fan, H.; Lopez, G. P. *Langmuir* **1997**, *13*, 119. (e) Gittins, D. I.; Bethell, D.; Nichols, R. J.; Schiffrin, D. J. *Adv. Mater.* **1999**, *11*, 737. (f) Chen, S. *Langmuir* **2001**, *17*, 2878.

(6) (a) Shipway, A. N.; Lahav, M.; Blonder, R.; Willner, I. *Chem. Mater.* **1999**, *11*, 13. (b) Patolsky, F.; Gabriel, T.; Willner, I. *J. Electroanal. Chem.* **1999**, *479*, 69. (c) Shipway, A. N.; Lahav, M.; Gabai, R.; Willner, I. *Langmuir* **2000**, *16*, 8789. (d) Lahav, M.; Shipway, A. N.; Willner, I.; Nielsen, M. B.; Stoddart, J. F. *J. Electroanal. Chem.* **2000**, *482*, 217. (e) Shipway, A. N.; Lahav, M.; Willner, I. *Adv. Mater.* **2000**, *12*, 993. (f) Shipway, A. N.; Willner, I. *Chem. Commun.* **2001**, 2035.

(7) (a) Porter, M. D.; Bright, T. B.; Allara, D. L.; Chidsey, C. E. D. *J. Am. Chem. Soc.* **1987**, *109*, 3559. (b) Bain, C. D.; Troughton, E. B.; Tao, Y.-T.; Evall, J.; Whitesides, G. M.; Nuzzo, R. G. *J. Am. Chem. Soc.* **1989**, *111*, 321. (c) Bryant, M. A.; Pemberton, J. E. *J. Am. Chem. Soc.* **1991**, *113*, 8284. (d) Chidsey, C. E. D. *Science* **1991**, *251*, 919. (e) Caldwell, W. B.; Campbell, D. J.; Chen, K.; Herr, B. R.; Mirkin, C. A.; Malik, A.; Durbin, M. K.; Dutta, P.; Huang, K. G. *J. Am. Chem. Soc.* **1995**, *117*, 6071. (f) Jung, H. H.; Won, Y. D.; Shin, S.; Kim, K. *Langmuir* **1999**, *15*, 1147. (g) Himmelhaus, M.; Eisert, F.; Buck, M.; Grunze, M. *J. Phys. Chem. B* **2000**, *104*, 576. (h) Han, S. W.; Lee, S. J.; Kim, K. *Langmuir* **2001**, *17*, 6981.

(8) (a) Nuzzo, R. G.; Allara, D. L. *J. Am. Chem. Soc.* **1983**, *105*, 4481. (b) Nuzzo, R. G.; Zegarski, B. R.; Dubois, L. H. *J. Am. Chem. Soc.* **1987**, *109*, 733. (c) Nuzzo, R. G.; Fusco, F. A.; Allara, D. L. *J. Am. Chem. Soc.* **1987**, *109*, 2358. (d) Offord, D. A.; John, C. M.; Griffin, J. H. *Langmuir* **1994**, *10*, 761.

(9) (a) Ogawa, H.; Chihara, T.; Taya, K. *J. Am. Chem. Soc.* **1985**, *107*, 1365. (b) Moskovits, M.; Suh, J. S. *J. Am. Chem. Soc.* **1985**, *107*, 6826. (c) Moskovits, M.; Suh, J. S. *J. Phys. Chem.* **1988**, *92*, 6327. (d) Tao, Y.-T. *J. Am. Chem. Soc.* **1993**, *115*, 4350. (e) Tao, Y.-T.; Lee, M.-T.; Chang, S.-C. *J. Am. Chem. Soc.* **1993**, *115*, 9547. (f) Thompson, W. R.; Pemberton, J. E. *Langmuir* **1995**, *11*, 1720. (g) Kim, S. H.; Ahn, S. J.; Kim, K. *J. Phys. Chem.* **1996**, *100*, 7174.

(10) (a) Reed, M. A.; Zhou, C.; Muller, C. J.; Burgin, T. P.; Tour, J. M. *Science* **1997**, *278*, 252. (b) Kohli, P.; Taylor, K. K.; Harris, J. J.; Blanchard, G. J. *J. Am. Chem. Soc.* **1998**, *120*, 11962. (c) Murty, K. V. G. K.; Venkataramanan, M.; Pradeep, T. *Langmuir* **1998**, *14*, 5446. (d) Rieley, H.; Kendall, C. K.; Zemicael, F. W.; Smith, T. L.; Yang, S. *Langmuir* **1998**, *14*, 5147. (e) Nakanishi, T.; Ohtani, B.; Uosaki, K. *J. Phys. Chem. B* **1998**, *102*, 1571. (f) Joo, S. W.; Han, S. W.; Kim, K. *J. Phys. Chem. B* **1999**, *103*, 10831. (g) Joo, S. W.; Han, S. W.; Kim, K. *J. Colloid Interface Sci.* **2001**, *240*, 391

10.1021/la026756o CCC: $25.00
Published on Web 07/09/2003

dithiols on a Au surface followed by reaction with gold nanoparticles, allowing the fabrication of nanostructured arrays.[11]

Aliphatic and aromatic diisocyanides are also known to adsorb on gold via only one NC group, with the other NC group pendent with respect to the gold surface.[12] This implies that nanostructured arrays can be assembled even using diisocyanides as the linker molecules. In those arrays, the Au−CN bond is supposed to exhibit higher electron conductance than the Au−SC bond since the atomic orbitals are conjectured to overlap more efficiently in the former bonding system than in the latter.[13] Aryl isocyanide thin films have thus attracted much attention, particularly due to their potential application as molecular wires.[14]

One of our research goals is to assemble effective nanoarrayed electrodes. This may be accomplished simply by attaching gold nanoparticles to a Au substrate by means of diisocyanide tethers. For example, by exposing a gold colloid monolayer to a solution of 1,4-phenylene diisocyanide (1,4-PDI), the cross-linker will assemble on the gold surface, leaving isocyanide moieties at the nanostructure−solution interface. The assembly of a second colloid layer will thereby be possible, and the construction can continue in the same way to produce colloid superstructures.[6] The overall conductivity will be dependent on the interparticle spacing as well as the size of the superstructure. As such, nanoarrayed superstructures can be assembled stepwise, but we are more interested in a one-step process to produce similar superstructures; for instance, a desired superstructure could be acquired by soaking a Au substrate into a gold sol solution containing 1,4-PDI. Some conditions may need to be satisfied, however, to control the quality of the superstructure, and this surely requires more detailed information on the nature of the adsorption scheme of 1,4-PDI on the colloidal Au particles.

In view of the above implications, we have conducted a surface-enhanced Raman scattering (SERS) study for 1,4-PDI in aqueous Au sol. In fact, the SERS spectra were highly dependent on the concentration of 1,4-PDI, and they were attributed to reflecting colloidal aggregates with different superstructures by referring to the supplementary data gathered from surface-enhanced infrared spectroscopy, UV/vis spectroscopy, transmission electron microscopy (TEM), atomic force microscopy (AFM), and quartz crystal microbalance (QCM).

2. Experimental Section

Preparation of Au Sol. The aqueous gold sol was prepared by following the procedures described in the literature:[15] 133.5 mg of $KAuCl_4$ (Aldrich) was initially dissolved in 250 mL of water, and the solution was brought to boiling. A solution of 1% sodium citrate (25 mL) was then added to the $KAuCl_4$ solution under vigorous stirring, and boiling was continued for ca. 20 min. The resulting purple solution showed the characteristic surface plasmon absorption band of nanosized gold particles at ca. 522 nm, and the average diameter of gold nanoparticles was determined to be 17 ± 1 nm from transmission electron microscope images; the final concentration of the Au sol solution was thus estimated to be 6.3×10^{-9} M. All the chemicals otherwise specified were reagent grade, and triply distilled water of resistivity greater than 18.0 MΩ·cm was used in making aqueous solutions.

Raman Spectral Measurement. Initially, to 0.96 mL of Au sol solution was added 0.04 mL of a methanol solution of 1,4-PDI (Aldrich, 5×10^{-2} to 1×10^{-5} M) using a micropipet to a final concentration ranging from 2×10^{-3} to 4×10^{-7} M. Subsequently, its Raman spectrum was obtained within 3∼5 min using a Renishaw Raman system 2000 spectrometer equipped with a holographic notch filter and an integral microscope (Olympus BH2-UMA). The 632.8 nm radiation from a 17 mW air-cooled He/Ne laser (Spectra Physics Model 127) was used as the excitation source. Raman scattering was detected with 180° geometry using a peltier-cooled (−70 °C) CCD camera (400 × 600 pixels). A glass capillary (KIMAX-51) with an outer diameter of 1.5−1.8 mm was used as a sampling device. The data acquisition time was 90 s. The holographic grating (1800 grooves/mm) and the slit permitted a spectral resolution of 1 cm^{-1}. The Raman band of a silicon wafer at 520 cm^{-1} was used to calibrate the spectrometer, and the accuracy of the spectral measurement was estimated to be better than 1 cm^{-1}. The Raman spectrometer was interfaced with an IBM-compatible PC, and the spectral data were analyzed using Renishaw WiRE software, version 1.2, based on the GRAMS/32C suite program (Galactic Industries).

Infrared Spectral Measurement. For a comparative study, surface-enhanced infrared absorption (SEIRA) spectroscopic measurement was conducted. The Au substrate with ca. 5 nm thickness was prepared by the resistive evaporation of gold (Aldrich, >99.99%) at 1×10^{-6} Torr on a trapezoid Si crystal (50 mm × 20 mm × 2 mm) that had been cleaned previously with ethanol in an ultrasonic cleaner; Au was coated only on one side of the silicon. The adsorption of 1,4-PDI on Au can be monitored by taking a series of SEIRA spectra after the Au/Si substrate has been in contact with a 1,4-PDI solution; the silicon crystal acts as the attenuated total reflection (ATR) element. However, since the Au film became unstable upon prolonged immersion in a 1,4-PDI methanolic solution, an alternative method, i.e., the drop-drying method, was adopted to see the adsorption of Au nanoparticles on 1,4-PDI/Au/Si substrates. In this method, an aliquot of 1 mM methanol solution of 1,4-PDI was spread on the gold film by using a micropipet, and the solvent was allowed to evaporate for 2 h in a closed chamber. After washing with methanol, the 1,4-PDI/Au/Si substrate was subjected to SEIRA analysis. After recording the SEIRA spectrum, the 1,4-PDI/Au/Si substrate was soaked in the Au sol solution (1.04×10^{-9} M) for a while; a low concentrated Au sol solution was used for the SEIRA spectra in order to have high *S*/*N* ratios. After washing several times with water to remove physisorbed Au nanoparticles, the substrate was subjected to SEIRA analysis in ambient conditions. Sometimes, the Au-particle-incorporated 1,4-PDI/Au/Si substrate was treated further with a methanolic solution of 1,4-PDI. Infrared spectra were measured using a Bruker IFS 113v Fourier transform IR spectrometer equipped with a Specac ATR attachment and a liquid N_2-cooled wide-band mercury cadmium telluride detector. The SEIRA spectrum was obtained by averaging 64 interferograms at 4 cm^{-1} resolution; the ATR−IR spectrum of a pure Au film on Si was taken as the reference. The incident angle of infrared light was set at 45° with respect to the plane of the silicon crystal such that 12 internal reflections in total took place throughout the crystal. The Happ−Genzel apodization function was used in Fourier transforming all the interferograms.

UV/Vis Spectral Measurement. UV/vis spectra were recorded for gold sols before and after the addition of 1,4-PDI using a SCINCO S-2130 spectrophotometer. The final concentration of 1,4-PDI added into the sol was the same as that in the concentration-dependent SERS measurement; one spectrum could be obtained within 3 s.

Transmission Electron Microscopy Measurement. TEM images were acquired for 1,4-PDI-containing gold sols using a JEM-200CX transmission electron microscope at 160 kV. The

(11) (a) Ohgi, T.; Sheng, H.-Y.; Nejoh, H. *Appl. Surf. Sci.* **1998**, *130−132*, 919. (b) Brust, M.; Bethell, D.; Kiely, C. J.; Schiffrin, D. J. *Langmuir* **1998**, *14*, 5425.

(12) (a) Robertson, M. J.; Angelici, R. J. *Langmuir* **1994**, *10*, 1488. (b) Irwin, M. J.; Jia, G.; Payne, N. C.; Puddephatt, R. J. *Organometallics* **1996**, *15*, 51. (c) Henderson, J. I.; Feng, S.; Ferrence, G. M.; Bein, T.; Kubiak, C. P. *Inorg. Chem. Acta* **1996**, *242*, 115. (d) Lin, S.; McCarley, R. L. *Langmuir* **1999**, *15*, 151. (e) Henderson, J. I.; Feng, S.; Bein, T.; Kubiak, C. P. *Langmuir* **2000**, *16*, 6183. (f) Horswell, S. L.; O'Neil, I. A.; Schiffrin, D. J. *J. Phys. Chem. B* **2001**, *105*, 941.

(13) Seminario, J. M.; Cruz, C. E. D. L.; Derosa, P. A. *J. Am. Chem. Soc.* **2001**, *123*, 5616.

(14) Chen, J.; Calvet, L. C.; Reed, M. A.; Carr, D. W.; Grubisha, D. S.; Bennett, D. W. *Chem. Phys. Lett.* **1999**, *313*, 741.

(15) Lee, P. C.; Meisel, D. *J. Phys. Chem.* **1982**, *86*, 3391.

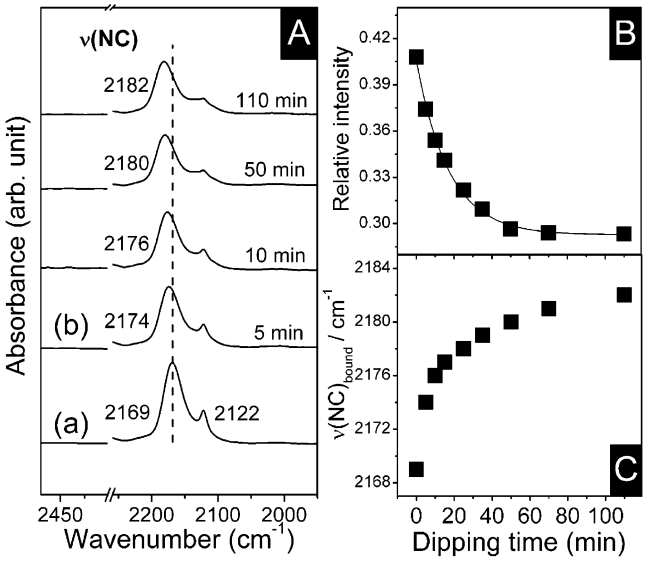

Figure 1. (A(a)) SEIRA spectrum of 1,4-PDI drop-and-dried on Au in the NC stretching region, and (A(b)) similar spectra taken after soaking the substrate in 1.04×10^{-9} M Au sol solution for 5−110 min. (B) Relative peak height of the $\nu(NC)_{free}$ and $\nu(NC)_{bound}$ bands in A(b) plotted against the immersion time of the 1,4-PDI/Au/Si substrate in Au sol solution. (C) Similar plot drawn to show the variation of the peak frequency of the $\nu(NC)_{bound}$ band.

sampling of the TEM measurement, i.e., dropping of 1,4-PDI-containing Au sols onto carbon-coated copper grids (150 mesh), was accomplished within 5 min after the addition of 1,4-PDI into Au sols; the final concentration of 1,4-PDI in the sol was the same as that in the concentration-dependent SERS measurement.

Atomic Force Microscopy Measurement. AFM images of Au films were obtained in air at room temperature by using a Digital Instruments Model Nanoscope IIIa scanning probe microscope. Using a V-shaped, 200 μm long Si_3N_4 cantilever with a nominal spring constant of 0.12 N/m (Nanoprobe, Digital Instruments), topography images were recorded in the conventional height mode (tapping mode, normal AFM) at a scan rate of 2−5 Hz.

Quartz Crystal Microbalance Measurement. To prepare a gold-coated quartz electrode, titanium (Aldrich, >99.99%) and gold (Aldrich, >99.99%) were consecutively evaporated onto an AT-cut quartz crystal (International Crystal Manufacture Co., fundamental resonance frequency, $f_o = 10$ MHz) at 1×10^{-6} Torr; the apparent area of the electrode was 0.2 cm^2. The details of the QCM apparatus were described previously.[16]

3. Results and Discussion

Infrared Spectral Features of 1,4-PDI on Gold. As mentioned in the Introduction, Robertson and Angelici[12a] concluded, with use of diffuse reflectance infrared Fourier transform (DRIFT) spectroscopy, that 1,4-PDI should adsorb on the gold surface via only one NC group, with the other NC group pendent with respect to the gold surface. To confirm such adsorption characteristics including the availability of the free isocyanide group for subsequent adsorption of colloidal Au particles, we have conducted a SEIRA spectroscopy study using a Au-coated silicone crystal as the ATR element. Figure 1A(a) shows a typical SEIRA spectrum in the region of 1950−2450 cm^{-1} for 1,4-PDI adsorbed on Au. Two peaks associated with the NC stretching vibration are clearly identified at 2122 and 2169 cm^{-1}. Although not shown here, for neat 1,4-PDI the NC stretching band is observed at 2132 cm^{-1} in the transmission infrared spectrum and at 2127 cm^{-1} in the ordinary Raman (OR) spectrum (see Figure 4a); they must be attributed, respectively, to the antisymmetric and symmetric stretching vibration of the diisocyanide groups.[17] The appearance of two NC stretching bands in the SEIRA spectrum implies that the two isocyanide groups of 1,4-PDI are no longer equivalent in the adsorbed state. The fact that one ν(NC) peak is strongly blue-shifted by 37 cm^{-1} from the position in a free state while the other peak is red-shifted by 10 cm^{-1} from that in a free state suggests that 1,4-PDI is adsorbed on gold mainly through one of the two isocyanide groups, as concluded by Robertson and Angelici.[12a] The blue-shift of the ν(NC) mode can be understood by invoking the fact that the carbon lone-pair electrons have antibonding character;[18] the donation of these electrons to gold should increase the strength of the NC bond. Considering that 1,4-PDI is a conjugated molecule, it is not unreasonable that a certain amount of red-shift in the one ν(NC) mode should occur.

The pendent NC group of 1,4-PDI is expected to react with Au nanoparticles. To confirm this, it will be desirable to take the SEIRA spectra in situ using an ATR cell. However, it took more than 7 h for the attainment of saturated coverage of 1,4-PDI on Au in 1 mM methanolic solution. Moreover, after soaking in methanolic solution for several hours, the evaporated gold was easily peeled off by a brief washing with methanol. Therefore, as described in the Experimental Section, the drop-drying method was employed to provide evidence on the layer-by-layer assembly of 1,4-PDI and Au nanoparticles on the Au/Si substrate. In Figure 1A(b) are shown the SEIRA spectra obtained after dipping in Au sol solution for different times ranging from 5 to 110 min; the actual SEIRA spectra were taken ex situ in ambient conditions. The peak due to the free NC group gradually loses its intensity as a function of the immersion time without a shift in its position. The intensity loss must be attributed to the anchoring of Au particles onto the pendent NC groups. As a result, the peak due to the Au-bonded NC group gradually blue-shifts from 2169 cm^{-1} up to 2182 cm^{-1}. Another noticeable observation is that the peak due to the free NC group hardly disappears even after prolonged soaking in Au sol solution. To see these spectral features more clearly, in Figure 1B is shown the variation of the relative peak height of the $\nu(NC)_{free}$ and $\nu(NC)_{bound}$ modes, $I_{NC(free)}/I_{NC(bound)}$, versus the immersion time in Au sol solution. A similar graph drawn for the peak frequency of the $\nu(NC)_{bound}$ mode is shown in Figure 1C. As can be seen from Figure 1B, the relative peak intensity decreases rapidly at the beginning upon immersing in the Au sol solution and then shortly attains a steady state; before immersing in the Au sol solution, the value of $I_{NC(free)}/I_{NC(bound)}$ is measured to be 0.41, but it becomes ∼0.29 after a prolonged immersion. The nonzero, steady-state value may indicate that the pendent NC groups cannot be covered fully with 17 nm-sized Au particles.[12f] This would also indicate that the majority of the Au nanoparticles were present as isolated single particles even after forming the Au−CN bonds; unbound NC groups might then be positioned between the Au nanoparticles (see AFM study section: to be discussed therein, the surface coverage of 1,4-PDI on Au/Si appeared to be ∼43% from the QCM measurement, and in turn, the maximum coverage of Au nanoparticles onto such a 1,4-PDI/Au/Si substrate seemed to be at best ∼14% from the AFM measurement; if we assume that the infrared absorption strength of the $\nu(NC)_{free}$ mode is only 0.41 times of that of the $\nu(NC)_{bound}$

(16) Han, S. W.; Ha, T. H.; Kim, C. H.; Kim, K. *Langmuir* **1998**, *14*, 6113.

(17) Han, H. S.; Han, S. W.; Kim, K. *Langmuir* **1999**, *15*, 6868.

(18) (a) Treichel, P. M. *Adv. Organomet. Chem.* **1973**, *11*, 121. (b) Singleton, E.; Oosthuizen, H. E. *Adv. Organomet. Chem.* **1983**, *22*, 130.

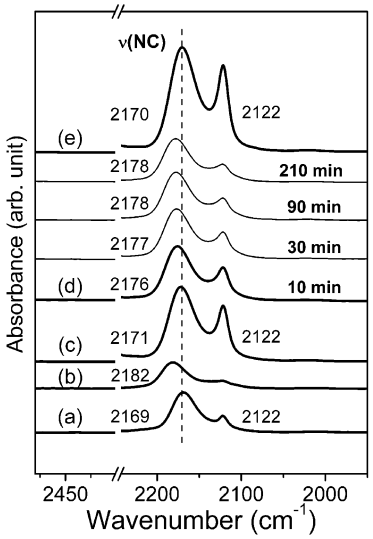

Figure 2. (a) SEIRA spectrum of 1,4-PDI on Au, and (b) similar spectrum taken after soaking the substrate in Au sol solution for 110 min (same as those in Figure 1A(b)). SEIRA spectra taken (c) after soaking the Au particle incorporated substrate into 1,4-PDI solution for a certain period of time, (d) after soaking subsequently in Au sol solution, and (e) after soaking once again in 1,4-PDI solution.

mode, the ratio of 0.29 measured above for $I_{NC(free)}/I_{NC(bound)}$ after a prolonged immersion must correspond to the 17% surface coverage of Au nanoparticles onto 1,4-PDI/Au/Si; this value is surprisingly close to that estimated from the AFM image). A similar observation was made when glass cover slips coated with mercaptopropyltrimethoxysilane were soaked in low concentrated Au or Ag colloid solution;[19] mercapto groups should bind to Au and Ag particles through a sulfur−metal bond.

Supposedly, 1,4-PDI molecules can be newly adsorbed on the Au nanoparticles that have previously been assembled on the 1,4-PDI/Au/Si substrate. Indeed, as can be seen from Figure 2c, distinct SEIRA spectral changes occurred following the adsorption of new 1,4-PDI molecules; for comparison, the SEIRA spectrum of 1,4-PDI assembled initially on the Au/Si substrate and that obtained after soaking in Au sol solution for 110 min are reproduced in Figure 2a,b, respectively. It can be seen that both the $\nu(NC)_{free}$ and $\nu(NC)_{bound}$ peaks show increased intensities, probably reflecting that the metal surface area has increased substantially upon the incorporation of gold nanoparticles. The other noteworthy point is that the maximum of the $\nu(NC)_{bound}$ peak is downshifted to 2171 cm^{-1}; the value is quite similar to that observed initially when 1,4-PDI is adsorbed on the vacuum-evaporated Au surface on Si. This may be rationalized by presuming that the number of 1,4-PDI molecules newly adsorbed on the Au nanoparticles is much larger than that adsorbed initially on the Au substrate. In addition, it is also conceivable that the transition dipole of the singly bound NC stretching mode is intrinsically greater than that of the α,ω-doubly bound NC stretching mode. In any case, as can be seen from Figure 2d, the peak due to the free NC group loses its intensity once again as the substrate is soaked in the Au sol solution. The peak due to the bound NC group also blue-shifts from 2171 cm^{-1} up to 2178 cm^{-1} upon treatment with the Au sol solution. Figure 2e shows the SEIRA spectrum recorded after the adsorption of additional 1,4-PDI on such a substrate. The spectral feature is indeed comparable to that of Figure 2c. These observations clearly suggest that nanoarrayed electrodes can be fabricated using 1,4-PDI as the conducting wires of Au nanoparticles.

Atomic Force Microscopy Image of Au Nanoparticles. Prior to presenting the AFM images, it will be informative to refer to the QCM data. When a Au-coated quartz electrode was dipped in 1 mM methanol solution of 1,4-PDI for 1 h, the QCM frequency change was measured to be 10 Hz; in the early stage of self-assembly, the frequency change is quite rapid but shortly it attains a near-plateau value up to 1 h. When the frequency change is transformed into a mass increase by referring to the Sauerbrey equation,[20] the mass increase corresponds to the 43.6% coverage of 1,4-PDI on Au; in this estimation, we presumed that 1,4-PDI is adsorbed on Au with a perpendicular orientation occupying an area of 21.1 $Å^2$ (6.4 Å × 3.3 Å);[21] as mentioned in the previous section, it takes more than 7 h for the attainment of saturated coverage of 1,4-PDI on Au in 1 mM methanolic solution. On these grounds, we show in Figure 3a,b the AFM images of a bare Si wafer and a Au surface evaporated thereon, respectively. The evaporated Au film is seen to have nanostructures with a domain size of ∼150 nm; the SEIRA substrate is supposed to have similar nanostructures. Similarly in the SEIRA experiment, 1,4-PDI was adsorbed on the Au/Si by a drop-drying method. The substrate was subsequently dipped in ∼1 nM Au sol solution, and the AFM images were collected thereafter. As can be seen in Figure 3c,d, Au nanoparticles were indeed adsorbed on the 1,4-PDI/Au/Si substrate. According to the line scan analysis, the height of the film varied from ∼14 nm to ∼38 nm (see the scale bar in Figure 3c,d). The distortion of the lateral resolution is supposed to arise from the AFM tip-induced broadening. Upon increasing the dipping time, the surface coverage of Au nanoparticles seemed to increase from ∼2% to ∼14% (see Figure 3e).[22] The surface coverage did not increase further, however, for up to 3 h. Several similar studies have already been reported that films covered more than 15% with metal nanoparticles is hardly achieved probably due to the repulsive forces between the surface-confined nanoparticles and the free nanoparticles in the solution.[23]

Raman Spectral Feature of 1,4-PDI on Gold Film. Figure 4b shows the SERS spectrum of 1,4-PDI adsorbed on Au nanoparticles supported on a glass slide; Au sol was spread on a glass slide, and then solvent was allowed to evaporate to obtain SERS-active Au film;[24] 40 μL of 1,4-PDI (3.2×10^{-4} M) was dropped onto the Au film, and upon drying the film was washed with methanol for the subsequent SERS measurement. For comparison, in Figure 4a is shown the OR spectrum of neat 1,4-PDI. The four distinct SERS peaks at 2161, 1595, 1202, and 1164 cm^{-1} in Figure 4b can be correlated with those at 2127 (ν(NC)), 1604 (8a), 1195 (7a), and 1172 (9a) cm^{-1} in Figure 4a. The weak peak at 1506 cm^{-1} in Figure 4b seems to be

(19) Maxwell, D. J.; Emory, S. R.; Nie, S. *Chem. Mater.* **2001**, *13*, 1082.

(20) Sauerbrey, G. *Z. Phys.* **1959**, *155*, 206.

(21) Ulman, A. *Acc. Chem. Res.* **2001**, *34*, 855.

(22) The surface coverage is estimated by manually counting the number of Au nanoparticles present in the AFM images (1 μm × 1 μm); the number of Au nanoparticles is counted to be 263 in Figure 3d. Since the effective area of those Au nanoparticles will be [263 × (2.27×10^{-16} $m^2/Au_{17\,nm}$)] = 5.97×10^{-14} m^2, the surface coverage is determined to be [(5.97×10^{-14} m^2)/(1 μm^2)][100/43.6] × 100 = 13.7%; herein, we also take account of the surface coverage of 1,4-PDI on Au to be 43.6%.

(23) (a) Brown, K. R.; Lyon, L. A.; Fox, A. P.; Reiss, B. D.; Natan, M. J. *Chem. Mater.* **2000**, *12*, 314. (b) Schmitt, J.; Mächtle, P.; Eck, D.; Möhwald, H.; Helm, C. A. *Langmuir* **1999**, *15*, 3256. (c) Sagara, T.; Kato, N.; Nakashima, N. *J. Phys. Chem. B* **2002**, *106*, 1205.

(24) Dick, L. A.; McFarland, A. D.; Haynes, C. L.; Van Duyne, R. P. *J. Phys. Chem. B* **2002**, *106*, 853.

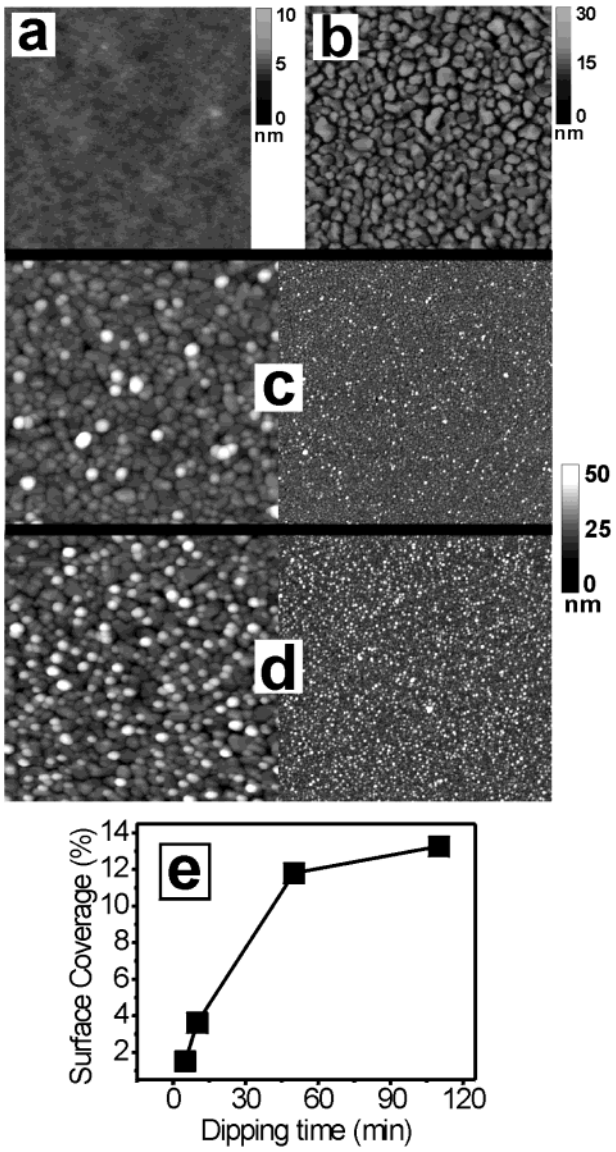

Figure 3. Tapping-mode AFM images (1 μm × 1 μm) of (a) bare Si wafer and (b) Au evaporated thereon. Representative 1 μm × 1 μm (left) and 5 μm × 5 μm (right) tapping-mode AFM images of a 17-nm Au nanoparticle adsorbed on the 1,4-PDI/Au/Si substrate for (c) 5 min and (d) 110 min in ~1 nM Au sol solution. (e) Surface coverage of the Au nanoparticles drawn versus the immersion time in the Au sol solution.

assigned to the Raman-inactive benzene ring 19a mode.[17] The appearance of such a mode in the SERS spectrum has to be attributed to the disruption of the symmetry of 1,4-PDI caused by surface adsorption. It is seen in the SERS spectrum that the ν(NC) peak is substantially broader than its counterpart in the OR spectrum. The peak position of the ν(NC) band in the SERS spectrum is 34 cm^{-1} higher than that in the OR spectrum. This is obviously due to the interaction of 1,4-PDI with the gold via the lone-pair electrons of the carbon atom and is in conformity with the infrared observation. Nonetheless, it is intriguing that the ν(NC) mode of the uncoordinated isocyanide group is not resolved in the SERS spectrum of 1,4-PDI. This does not seem to indicate, however, that 1,4-PDI molecules are lying flat on the gold surface. According to the electromagnetic (EM) selection rule,[25] vibrational modes whose polarizability tensor elements

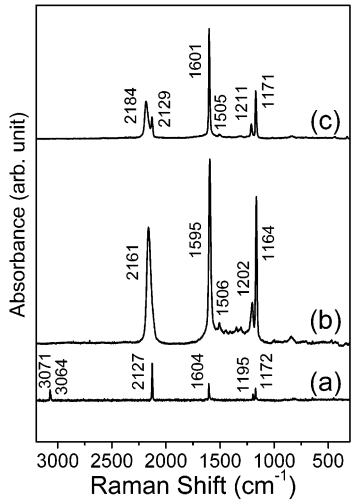

Figure 4. (a) OR spectrum of neat 1,4-PDI. (b) SERS spectrum of 1,4-PDI on Au film. (c) SERS spectrum of 1,4-PDI (8×10^{-5} M) in Au sol.

are perpendicular to a metal surface should be strongly enhanced in an SERS spectrum, namely, those corresponding to α'_{zz}, where z is along the surface normal. Vibrations derived from α'_{xz} and α'_{yz} should be the next most intense modes, while those corresponding to α'_{xx}, α'_{yy}, and α'_{xy} are less enhanced. On these grounds, with an upright orientation of 1,4-PDI on gold, the most intense bands in the SERS spectrum will be derived from the A_g-type modes. Bands belonging to the B_{2g} and B_{3g} symmetries will be the next most intense ones. In fact, the distinctly observed SERS peaks in Figure 4b, i.e., 7a, 8a, and 9a, are all attributable to the A_g bands.[17] Although this may not necessarily mean that the adsorbate must have a perfectly perpendicular orientation on the gold surface, the possibility of the existence of a flat reclining structure is strongly rejected. One plausible reason for the absence of the $\nu(NC)_{free}$ band in Figure 4b will be discussed in a later section.

Raman Spectral Features of 1,4-PDI in Gold Sol Solution. The "as-prepared" Au sol solution exhibited an absorption maximum at ca. 522 nm in the UV/vis spectrum.[15] Upon the addition of an aliquot amount of 1,4-PDI, the peak shifts to 528 nm with lowered intensity. At the same time, a very strong absorption band develops around 700 nm. As will be discussed further below, this indicates that 1,4-PDI molecules induce the aggregation of Au nanoparticles by forming Au−C bonds.[26] It is thus expected that strong SERS enhancement will occur for 1,4-PDI dissolved in aqueous Au solution. On these grounds, in Figure 4c is shown the SERS spectrum of 1,4-PDI in a Au sol solution; the concentration of 1,4-PDI was 8×10^{-5} M. Assuming that 1,4-PDI molecules adsorb perpendicularly on the 17 nm-sized Au sol particles, the concentration needed for full coverage is estimated to be 2.6×10^{-5} M;[27] if two isocyanide groups of 1,4-PDI are bonded independently to two different Au particles, 1.3×10^{-5} M will be sufficient for full coverage. In light of this, the concentration used to record the SERS spectrum in Figure 4c must be above the full-coverage limit. Nonetheless, it has to be mentioned that the concentration is too low to observe the OR spectrum of 1,4-PDI. This implies that all the peaks in Figure 4c must be attributed to 1,4-PDI adsorbed on the Au sol surface; that is, the spectrum must be an SERS spectrum. Once again, the

(25) (a) Creighton, J. A. *Surf. Sci.* **1983**, *124*, 209. (b) Moskovits, M. *Rev. Mod. Phys.* **1985**, *57*, 783.

(26) Storhoff, J. J.; Elghanian, R.; Mucic, R. C.; Mirkin, C. A.; Letsinger, R. L. *J. Am. Chem. Soc.* **1998**, *120*, 1959.

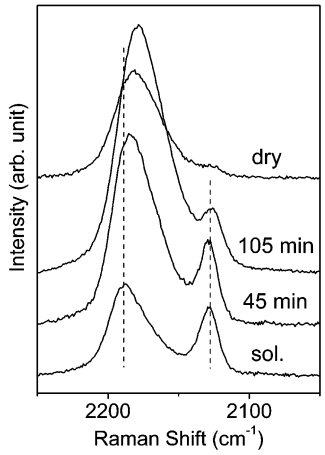

Figure 5. SERS spectra of a droplet of 1,4-PDI recorded following the solvent evaporation. The initial concentration of the drop was 8×10^{-5} M.

distinct peaks at 1601, 1211, and 1171 cm^{-1} can be assigned to the ring 8a, 7a, and 9a modes, respectively. It is intriguing that two peaks are identified in the region of the NC stretching vibration, one at 2184 cm^{-1} and the other at 2129 cm^{-1}. The former peak must be due to the isocyanide group bonded to the Au sol surface, while the latter peak is associated with the terminal, pendent isocyanide group.

It is very intriguing that the $\nu(NC)_{free}$ band is clearly identified in the sol state, whereas it is hardly detected in the film state (see Figure 4b,c). Recalling the SEIRA observation, a free isocyanide group must be present even in the film state, however. To resolve the difficulty, we have monitored the SERS spectral changes that occur for a drop of 1,4-PDI-containing sol upon drying to give a film. As can be seen in Figure 5, the $\nu(NC)_{bound}$ band becomes intensified as the solvent evaporates; this is probably due to the formation of more SERS-active Au aggregates. The $\nu(NC)_{bound}$ band is also subjected to a noticeable red-shift along with a substantial band broadening. Concomitantly, the $\nu(NC)_{free}$ band is gradually weakened, and it finally becomes barely detectable in the fully dried state. The re-immersion of the film into H_2O or methanol media does not induce any further SERS spectral change; the process is thus irreversible and quite reproducible. This implies that the initial spectral feature showing two separate isocyanide peaks is not recovered. This indicates that the activation barrier is significant for 1,4-PDI in the film state to return to that corresponding to the initial sol state. Although the detailed nature of the process is a matter of conjecture, it is conceivable that in the sol state, 1,4-PDI molecules are rather mobile due to the intervention of solvent and/or electrolyte species, but in the film state, 1,4-PDI molecules assume a rigid aggregate due to the stronger interring $\pi-\pi$ interaction; once a rigid aggregate is formed, it is difficult to separate them into mobile molecules. The absence of the $\nu(NC)_{free}$ band in the SERS spectrum in the film state seems thus to be attributed to the inhomogeneous broadening of the $\nu(NC)_{bound}$ band caused by the fractal Au substrate; we can notice that the $\nu(NC)$ band in Figure 4b is in fact asymmetric toward the low-frequency region. In conjunction with this, it will be helpful to refer to our earlier work on the adsorption of 1,4-PDI on powdered Ag substrate.[17] It has been found previously that 2 μm sized Ag particles are very efficient substrates for the infrared and Raman spectroscopic characterization of molecular adsorbates.[28] The diffuse reflectance infrared Fourier transform (DRIFT) spectrum is observed to be little different from the reflection−absorption infrared (RAIR) spectrum taken for the same molecules on flat silver films. The Raman spectrum on the other hand is a SERS spectrum, exhibiting little difference from that taken on vacuum-evaporated thin, rough silver films. In fact, in the DRIFT spectrum of 1,4-PDI adsorbed on 2μm sized Ag particles, both the $\nu(NC)_{bound}$ and $\nu(NC)_{free}$ bands were clearly identified, whereas in the Raman spectrum, however, $\nu(NC)_{free}$ band was hardly detected, as similarly in the present work.

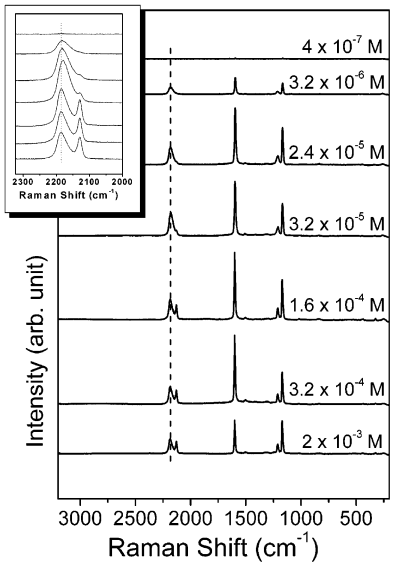

Figure 6. Concentration-dependent SERS spectra of 1,4-PDI in Au sol, ranging from 4×10^{-7} to 2×10^{-3} M. The inset shows the enlarged view of the NC stretching region.

Concentration-Dependent SERS Spectra of 1,4-PDI in Gold Sol Solution. In Figure 4c we have noticed that both the free and bound isocyanide groups can be present simultaneously when the adsorbate concentration is above the full-coverage limit. It is conceivable that the number of free isocyanide groups available will diminish when the adsorbate concentration is lowered to the submonolayer-coverage limit. This would be confirmed from the analysis of the concentration-dependent SERS spectra. In this respect, a series of SERS spectra were taken using Au sol solutions containing 1,4-PDI from 4×10^{-7} to 2×10^{-3} M, and they are shown in Figure 6. As approximated previously, in an ideal case, a free isocyanide group will not be present if the concentration of 1,4-PDI is below 1.3×10^{-5} M. Indeed, the $\nu(NC)_{free}$ peak is seen to be very weak in the SERS spectrum taken at $<2.4 \times 10^{-5}$ M; see the inset of Figure 6.

Figure 7a shows the relative peak intensity of the $\nu(NC)_{free}$ and $\nu(NC)_{bound}$ bands in Figure 6 plotted against the concentration of 1,4-PDI in the Au sol solution. Figure 7b shows the variation of the peak position of the

(27) The concentration of 1,4-PDI needed to cover the Au nanoparticles present in 0.96 mL of 6.3 nM Au sol is calculated as follows. Using the average diameter of Au nanoparticles, 17 nm, determined from the TEM image, the mean surface area and volume of a single particle are estimated to be 907.9 nm^2 and 2572 nm^3, respectively. Assuming then that each 1,4-PDI occupies an area of 21.1 $Å^2$ (6.4 Å × 3.3 Å)[21] on a gold surface, the number of 1,4-PDI molecules needed to cover one single nanoparticle will be 4302. Since the number of Au nanoparticles present in 0.96 mL of 6.3 nM Au sol is presumed to be 3.64×10^{12}, the number of 1,4-PDI molecules to cover all these nanoparticles is estimated to be 1.57×10^{16}; $[(4302) \times (3.64 \times 10^{12})] = 1.57 \times 10^{16}$. Then, the concentration of 1,4-PDI needed for a full-coverage limit in 1 mL solution will be 2.6×10^{-5} M.

(28) Han, S. W.; Han, H. S.; Kim, K. *Vib. Spectrosc.* **1999**, *21*, 133.

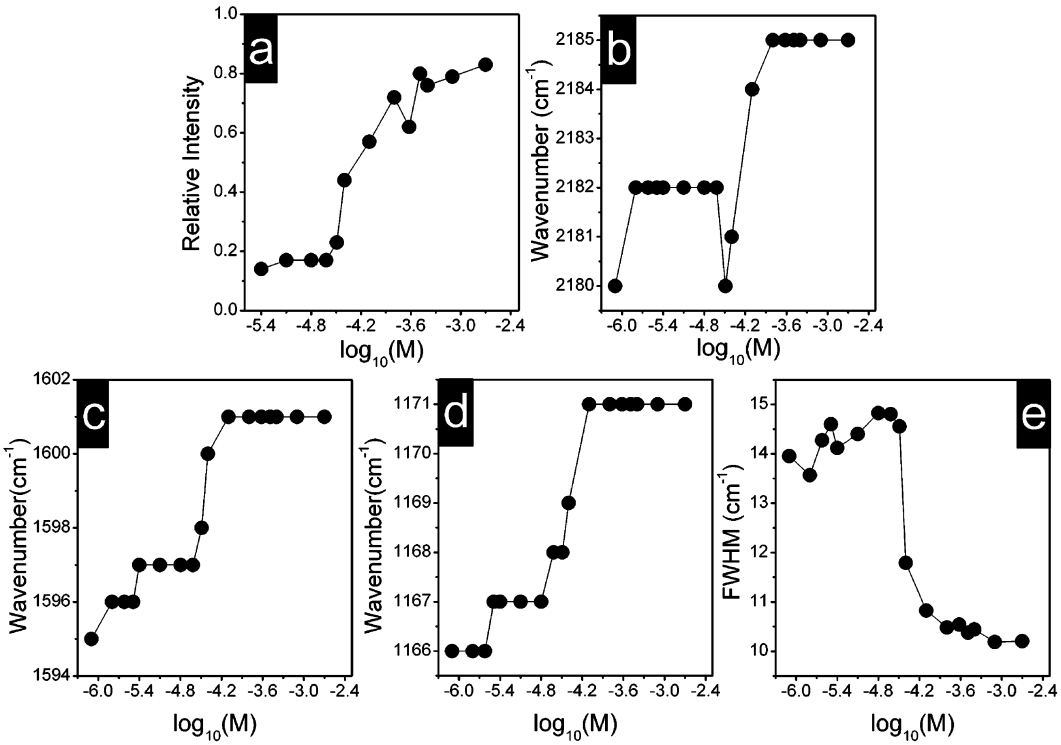

Figure 7. (a) Relative intensity of the $\nu(NC)_{free}$ and $\nu(NC)_{bound}$ bands in Figure 6 plotted against the concentration of 1,4-PDI in the Au sol solution. (b) Similar plot drawn to show the variation of the peak frequency of the $\nu(NC)_{bound}$ mode. Peak positions of the ring (c) 8a and (d) 9a modes in Figure 6 plotted against the concentration of 1,4-PDI in the Au sol solution. (e) Bandwidth of the ring 8a mode in Figure 6 plotted against the concentration of 1,4-PDI in the Au sol solution.

$\nu(NC)_{bound}$ band similarly plotted against the 1,4-PDI concentration. In fact, the relative peak intensity varies with a sigmoid shape, and the inflection point is found to be near 3.2×10^{-5} M. Below the latter concentration, the two isocyanide groups in 1,4-PDI must have bonded to gold particles, whereas the free isocyanide group is available above the inflection point; the somewhat higher value, 3.2×10^{-5} M, than the theoretical one, 1.3×10^{-5} M, is presumed due to the dynamic equilibrium between the adsorbed 1,4-PDI molecules and the unadsorbed ones in the sol medium. At a concentration above 10^{-3} M, the relative peak intensity is seen to attain a plateau value of ~0.8. This may indicate that, at higher concentration, a fair number of 1,4-PDI molecules are bound to gold nanoparticles via only one of its two isocyanide groups; it is conceivable that, at higher concentration, newly added 1,4-PDI molecules cannot cross-link different nanoparticles since only a limited space is available between nanoparticles. It is also noteworthy in Figure 7b that a minimum is reproducibly observed at 3.2×10^{-5} M. At 3.2×10^{-5} M, the $\nu(NC)_{bound}$ peak appears at 2180 cm^{-1}, but below this concentration, the peak is observed at 2182 cm^{-1}. At higher concentrations, i.e., $>1.6 \times 10^{-4}$ M, the peak appears at 2185 cm^{-1}. These observations strongly suggest that the adsorption scheme of 1,4-PDI onto Au nanoparticles must change dramatically at a concentration near the monolayer-coverage limit, i.e., 3.2×10^{-5} M. At lower concentrations, 1,4-PDI is bound to two different gold particles. Upon increasing the concentration, the surface coverage gradually increases with the increase of the pendent isocyanide groups but not affecting the cross-linked 1,4-PDI already present. It is a reasonable presumption that donation of the carbon lone-pair electrons to Au should be more substantial when forming one Au−C bond than in the case of forming two Au−C bonds. Therefore, the peak frequency of the $\nu(NC)_{bound}$ is higher at higher concentration than at lower concentration.

If the adsorption scheme is dependent on the adsorbate concentration, the SERS spectral features of the benzene ring modes are also expected to change as a function of the 1,4-PDI concentration. This is indeed confirmed from the variation of the peak frequency of the ring modes. In Figure 7c,d are shown the SERS peak positions of the ring 8a and 9a modes plotted against the concentration of 1,4-PDI in the Au sol solution. For both cases, the peak positions showed changes with a sigmoid shape. The inflection points were also seen to be near 3.2×10^{-5} M as in the case of the $\nu(NC)_{bound}$ mode. Once again, the peak frequencies of the 8a and 9a modes are also invariant when the concentration is kept above 1.6×10^{-4} M. Although not shown here, the peak frequency of the ring 7a mode is also varied as a function of 1,4-PDI concentration. The peak frequencies attained plateau values at low and high concentration regions. Surprisingly, a minimum is also identified reproducibly (for the ring 7a mode) at a concentration of 3.2×10^{-5} M. This feature is the same as that observed for the $\nu(NC)_{bound}$ band shown in Figure 7b.

Not only the peak position but also the bandwidth is also a very useful spectral parameter. As shown in Figure 7e, the bandwidth of the ring 8a mode also varies as a function of the 1,4-PDI concentration. It has to be mentioned that the bandwidth of the 8a mode is at best ~7 cm^{-1} in the OR spectrum (in highly crystalline state), but the value is in fact seen to be 10−15 cm^{-1} in the SERS spectra. The inflection point in Figure 7e is situated once again near 3.2×10^{-5} M. At lower concentration, the bandwidth is as much as 15 cm^{-1}, while at higher concentration it amounts to 10 cm^{-1}. Although one may attribute such a band broadening to surface−ring π orbital interaction, such a possibility is very low. Considering that 1,4-PDI is a conjugated molecule, the inductive effect will be significant when the molecule adsorbs on metal surfaces.[29] The higher bandwidth at low concentration is

Chart 1. Plausible Scheme for the Adsorption of 1,4-PDI on Gold Nanoparticles in Aqueous Medium

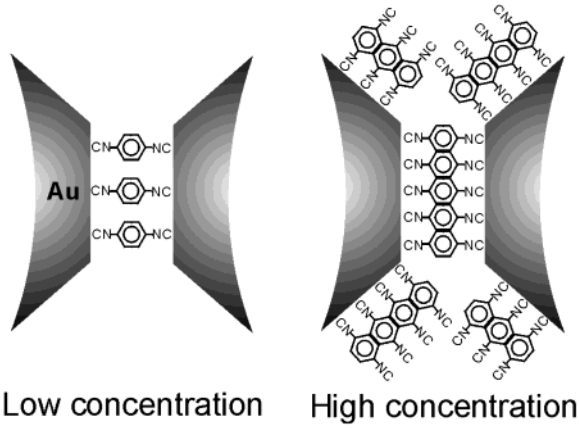

simply due to the formation of two Au−C bonds. At higher concentration, the bandwidth will be small since the newly adsorbing 1,4-PDI molecules are bound to Au via only one of its two isocyanide groups due to the limited space available to cross-link different nanoparticles; the appearance of the $\nu(NC)_{free}$ band at 2129 cm^{-1} in the SERS spectra as well as the fast aggregation of Au particles at higher 1,4-PDI concentration (vide infra) supports the present argument. Accordingly, all SERS spectral changes associated with the benzene ring modes must be attributed to the changes in the adsorption scheme of 1,4-PDI on Au particles. On these grounds, the plausible adsorption scheme of 1,4-PDI on gold nanoparticles is drawn in Chart 1.

It also should be mentioned that the Au colloids eventually settle out into two separate phases. When the added concentration of 1,4-PDI was very high, i.e., $>10^{-4}$ M, precipitates were formed about 10 min later after the addition of 1,4-PDI into the sol solution; a much longer time was needed for precipitates to form in dilute conditions. Even though precipitates are formed, the SERS spectral pattern of the sol itself is invariant; nonetheless, the EF diminishes considerably. However, the SERS spectral feature of the dried precipitates was barely dependent on the initial concentration of 1,4-PDI in the Au sol solution (data not shown). The $\nu(NC)_{bound}$ band was found distinctly at 2170−2180 cm^{-1}, but the $\nu(NC)_{free}$ band was not detected at all in the spectrum. In addition, the peak positions of the ring 8a and 9a modes were also very close to those observed in the sol SERS spectra taken at a very low concentration of 1,4-PDI. These spectral data suggest that the precipitates are in fact nanoarrayed superstructures consisting of Au nanoparticles linked by 1,4-PDI molecules through the formation of two Au−C bonds.

UV/Vis Spectra and TEM Images of Au Sol. In conjunction with the aggregation of Au nanoparticles by 1,4-PDI, a series of UV/vis absorption spectra were obtained as a function of time after adding 1,4-PDI into the Au sol solution; the final concentration of 1,4-PDI was the same as that used in the SERS measurement. It was confirmed at first that the addition of 0.02 mL of methanol to 0.48 mL of Au sol does not influence the UV/vis absorption spectral feature of the sol for up to 1 h; in the SERS measurement, we added a 1,4-PDI solution into Au sol with the same volume ratio. Hence, any UV/vis spectral change occurring after the addition of 1,4-PDI must be attributed to the interaction of 1,4-PDI with Au nanoparticles.

(29) Gao, P.; Weaver, M. J. *J. Phys. Chem.* **1985**, *89*, 5040.

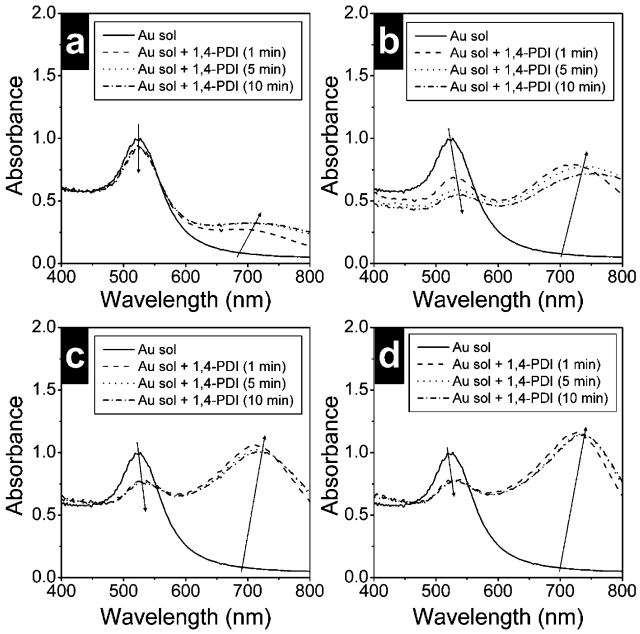

Figure 8. UV/vis spectra of Au sol after the addition of 1,4-PDI with the final concentration of (a) 4.0×10^{-6}, (b) 1.6×10^{-5}, (c) 3.2×10^{-5}, and (d) 3.2×10^{-4} M.

Figure 8 shows that the time-dependent optical spectra of a Au sol solution after the addition of 1,4-PDI. Consulting the previous estimation that the concentration needed for the full coverage of 1,4-PDI on nanoparticles is 2.6×10^{-5} M, four different concentrations were chosen to follow the aggregation of Au nanoparticles: 4.0×10^{-6} M (below 2.6×10^{-5} M), 1.6×10^{-5} and 3.2×10^{-5} M (near 2.6×10^{-5} M), and 3.2×10^{-4} M (over 2.6×10^{-5} M) of 1,4-PDI. In fact, for all cases, a broad surface plasmon band has developed in the region of 650−800 nm; this indicates the formation of Au clusters and/or aggregates with longitudinal axes.[30] Specifically, at 4.0×10^{-6} M (Figure 8a), a relatively slow aggregation seemed to proceed along with a slight decrease in the absorption maximum at ∼522 nm. This implies that the Au clusters or aggregates are not large-sized at all. Recalling from the SERS spectral data that the $\nu(NC)_{free}$ band is hardly detected at 4.0×10^{-6} M, these small clusters must be composed of nanoparticles cross-linked by 1,4-PDI. As can be seen in Figure 9a, small-sized fractal clusters are in fact dominant in the corresponding TEM image; the completely isolated single particles are also seen in the image. This reflects that the adsorbate concentration, i.e., 4.0×10^{-6} M, is not high enough to reduce the repulsive barrier between Au particles covered by citrate anions. It is also a compelling fact that the formation of two Au−C bonds per 1,4-PDI is a thermodynamically favorable process. Another point worth considering is that the midpoint of two Au nanoparticles with a separation of ∼1 nm have frequently been claimed to be the "hot" site for SERS;[31] the size of 1,4-PDI is indeed ∼1 nm.

Upon increasing the 1,4-PDI concentration, UV/vis spectral changes took place more dramatically. At 1.6×10^{-5} M (Figure 8b), the initial plasmon band at ∼520 nm diminished more rapidly than at 4.0×10^{-6} M; the broad band at 720 nm also developed distinctly within 1 min. In fact, a highly aggregated superstructure is clearly identified in the corresponding TEM image shown in

(30) Bohren, C. F.; Huffman, D. R. *Absorption and Scattering of Light by Small Particles*; John Wiley & Sons: New York, 1983.

(31) Xu, H.; Aizpurua, J.; Käll, M.; Apell, P. *Phys. Rev. E* **2000**, *62*, 4318.

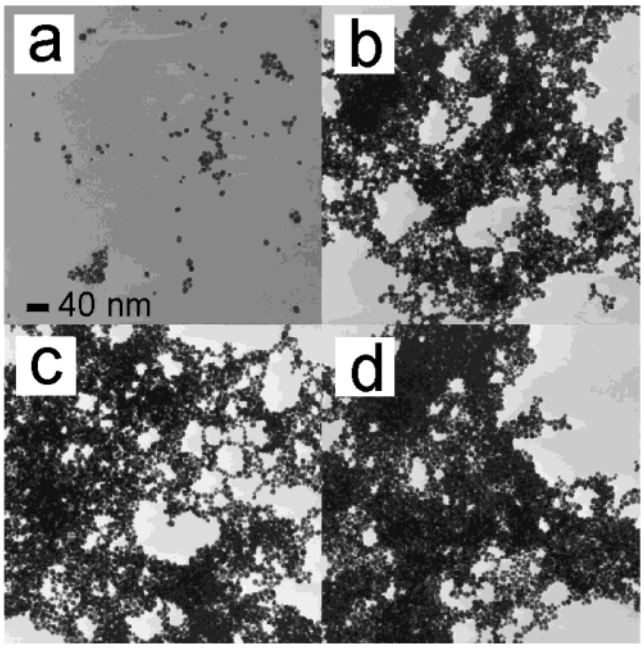

Figure 9. TEM images of Au sol after the addition of 1,4-PDI with the final concentration of (a) 4.0×10^{-6}, (b) 1.6×10^{-5}, (c) 3.2×10^{-5}, and (d) 3.2×10^{-4} M.

Figure 9b. Recalling the SERS data that only the $\nu(NC)_{bound}$ band is identified at 1.6×10^{-5} M, this may imply that the major driving force for Au nanoparticles to assemble large aggregates is the formation of two Au−C bonds per 1,4-PDI rather than the usual adsorbate-induced reduction of the electrical repulsive barrier between Au particles. At 3.2×10^{-5} M (Figure 8c) and 3.2×10^{-4} M (Figure 8d), both the decrease of the original 520 nm band and the development of the 720 nm band are completed within 1 min. This is indicative of the formation of highly aggregated superstructures that can also be confirmed from the TEM images shown in Figure 9c,d. We have already presumed that the formation of two Au−C bonds per 1,4-PDI is a thermodynamically favorable process. Then, the fact that not only the $\nu(NC)_{bound}$ band but also the $\nu(NC)_{free}$ band is clearly detected in the SERS spectrum at 3.2×10^{-5} M (as well as at 3.2×10^{-4} M) may indicate that ultimately there remains no interstitial site wherein 1,4-PDI can be bound by two Au nanoparticles; this corresponds to the situation of the right panel in Chart 1. Eventually, however, the UV/vis absorption becomes lost in all cases due to the formation of largely aggregated particles to precipitate; at lower concentration, it comparatively takes longer times.

According to the EM enhancement mechanism, the SERS intensity has to be correlated with the absorbance of the Au sol measured at the Raman excitation wavelength.[32] In this light, the UV/vis spectra taken at 3 and 5 min after the addition of 1,4-PDI into the Au sol are collectively shown in Figure 10a,b, respectively; it has to be remembered that the sol-SERS spectra were measured within 5 min after the addition of 1,4-PDI in Au sol. In addition, the normalized absorbance at the Raman excitation wavelength, i.e., at 632.8 nm, measured as a function of time after the addition of 1,4-PDI is drawn in Figure 10c, and the variations of the SERS intensity of the $\nu(NC)_{bound}$ band at four typical 1,4-PDI concentrations are drawn in Figure 10d. In fact, the absorbance at the

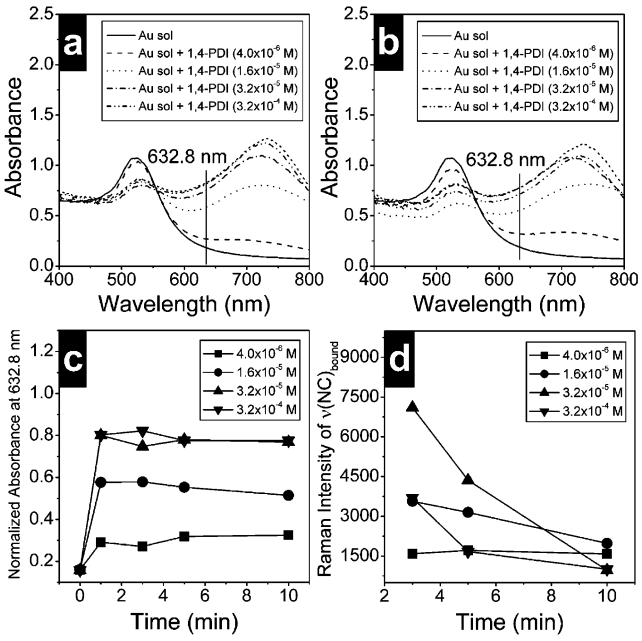

Figure 10. UV/vis spectra of Au sol measured (a) 3 min and (b) 5 min after the addition of 1,4-PDI at different concentrations. (c) Evolution of the absorbance of the 1,4-PDI added Au sol at the Raman excitation wavelength, i.e., 632.8 nm and (d) the corresponding variation of the SERS intensity of the $\nu(NC)_{bound}$ band.

Raman excitation wavelength is seen in Figure 10c to be higher at higher 1,4-PDI concentration. In accordance, the SERS intensity is seen in Figure 10d to be more intense at higher 1,4-PDI concentration, at least in the early stage of the addition of 1,4-PDI into the Au sol. All sol-SERS spectra in this work may then be correlated with the absorbance of the sol of interest at 632.8 nm. Nonetheless, the SERS intensity diminished substantially within 10 min, albeit that the absorbance at the Raman excitation wavelength was maintained during that time with negligible variation. This may indicate that the actual superstructure composed of 1,4-PDI and Au nanoparticles is subjected to ceaseless structural change not readily discernible from the optical absorption characteristics. Several authors have reported such an unexpected SERS intensity decrease for high concentrations of molecules adsorbed on metal colloids.[33] This is usually explained by a time-dependent aggregation of the colloidal substrate that leads to variations in the morphology of the aggregates.

4. Summary and Conclusion

We have investigated the adsorption characteristics of 1,4-PDI on colloidal Au particles by means of various analytical techniques. The SEIRA spectral data clearly showed that 1,4-PDI should be adsorbed on gold via the carbon lone-pair electrons of one isocyanide group assuming a vertical orientation with respect to the gold substrate. The pendent isocyanide group is further identified by SEIRA spectroscopy, AFM, and QCM to react with Au nanoparticles. The SEIRA spectroscopy also revealed that 1,4-PDI molecules could be newly adsorbed on those Au nanoparticles, implying that nanoarrayed electrodes could be fabricated using 1,4-PDI as the conducting wires of Au nanoparticles. Invoking the EM selection rule, the distinct appearance of the A_g-type bands

(32) Schatz, G. C.; Van Duyne, R. P. In *Handbook of Vibrational Spectroscopy*; Griffiths, P. R., Ed.; John Wiley & Sons: New York, 2001; p 1.

(33) Procházka, M.; Štěpánek, J.; Turpin, P.-Y.; Bok, J. *J. Phys. Chem. B* **2002**, *106*, 1543.

in the SERS spectrum on Au film must also reflect an upright orientation of 1,4-PDI on gold although the ν(NC) mode of the uncoordinated isocyanide group is not resolved in the SERS spectrum. In the Au sol medium, the actual structure of the composite is highly dependent on the concentration of 1,4-PDI. The "as-prepared" Au sol solution exhibits an absorption maximum at 520 nm in the UV/vis spectrum, but upon the addition of a small amount of 1,4-PDI, a very strong absorption band develops around 700 nm, indicating the aggregation of Au nanoparticles by forming Au−C bonds. In the SERS spectra, the relative peak intensity of the $\nu(NC)_{free}$ and $\nu(NC)_{bound}$ modes varied with a sigmoid shape with respect to the 1,4-PDI concentration. The inflection point was situated at $\sim 3.2 \times 10^{-5}$ M, which was surprisingly close to that of the monolayer-coverage limit. The adsorption scheme of 1,4-PDI on Au nanoparticles thus seemed to change dramatically near the inflection point. At lower concentration below IP, the 1,4-PDI molecules appear to be bonded exclusively to two different gold particles forming two Au−C bonds. The resulting fractal clusters are rather small-sized, however, because of the repulsive barrier between Au particles at lower concentration. At higher concentration above IP, a highly aggregated superstructure is readily formed, showing both the $\nu(NC)_{free}$ and $\nu(NC)_{bound}$ bands in the SERS spectra. The peak positions as well as the bandwidths of the benzene ring modes also varied similarly to the case of the ν(NC) mode with respect to the 1,4-PDI concentration, implying that all SERS spectral changes associated with the benzene ring modes must have been caused by the change in the adsorption scheme of 1,4-PDI onto Au particles. The observations made by SERS, UV/vis spectroscopy, and TEM suggest altogether that the major driving force for Au nanoparticles to assemble large aggregates is presumably the formation of two Au−C bonds per 1,4-PDI rather than the usual adsorbate-induced reduction of the electrical repulsive barrier between Au particles.

Acknowledgment. This work was supported in part by the Ministry of Health & Welfare (Korea Health 21 R&D Project, 01-PJ11-PG9-01NT00-0023), the Ministry of Science and Technology (Korea Nano Core Basis Project, M10213240001-02B1524-00210) of the Republic of Korea, and the Korea Science and Engineering Foundation (KOSEF, 1999-2-121-001-5). H.S.K. is also supported by KOSEF through the Center for Molecular Catalysis at Seoul National University. N.H.K. and H.K.P. are recipients of the BK21 fellowship.

LA026756O